Fibers and Polymers 2017, Vol.18, No.11, 2049-2059
DOI 10.1007/s12221-017-1175-9

ISSN 1229-9197 (print version)
ISSN 1875-0052 (electronic version)

Crystallization Behavior, Rheology, Mechanical Properties, and Enzymatic Degradation of Poly(L-lactide)/Poly(D-lactide)/Glycidyl Methacrylate Grafted Poly(ethylene octane) Blends

Xiangyu Yan[1,2], Yan Zhao[3], Yanping Hao[1], Hongwei Pan[1], Huiliang Zhang[1]*, Zhe Wang[2], and Lisong Dong[1]

[1]*Key Laboratory of Polymer Ecomaterials, Chinese Academy of Sciences, Changchun Institute of Applied Chemistry, Changchun 130022, P. R. China*
[2]*Synthetic Resins and Special Fiber Engineering Research Center, Ministry of Education, Changchun University of Technology, Changchun 130012, P. R. China*
[3]*State Key Laboratory of Molecular Engineering of Polymers, Collaborative Innovation Center of Polymers and Polymer Composite Materials, Department of Macromolecular Science, Laboratory of Advanced Materials, Fudan University, Shanghai 200433, P. R. China*

(Received December 1, 2016; Revised July 25, 2017; Accepted September 9, 2017)

Abstract: Poly(L-lactide) (PLLA)/poly(D-lactide) (PDLA)/poly(ethylene octene) grafted with glycidyl methacrylate (GPOE) were prepared by simple melt blending method at PDLA loadings from 1 to 5 wt%. Differential scanning calorimetry (DSC) and wide-angle X-ray diffraction (WAXD) demonstrated the formation of the stereocomplex in the blends. The addition of PDLA led to the increase of nucleation density from polarized microscope (POM) observations. Rheological measurements indicated that the blends exhibited a rheological fluid-solid transition and an enhanced elastic behavior in that ternary system as the PDLA loadings reached up to 5 wt%. By adding 1-2 wt% PDLA, the ternary system has better tensile and impact properties. Dynamic Mechanical Analysis (DMA) results showed that SC crystal formation and its effect on the enhancement of thermal stability at higher temperature. It is interesting that the enzymatic degradation rates have been enhanced clearly in the PLLA/PDLA/GPOE blends than in the PLLA/GPOE blend, which may be of great use and significance for the wider practical application of PLLA/GPOE blends.

Keywords: Poly(L-lactide), Poly(D-lactide), Poly(ethylene octene), Rheological, Enzymatic degradation

Introduction

As more and more countries and states follow in banning plastic grocery bags responsible for so-called "white pollution" around the world, bioplastics is poised to play a big role as a viable, biodegradable replacement [1]. Poly(lactic acid) (PLA) is a biodegradable polymer that can be available from agricultural renewable resources [2]. It is an aliphatic thermoplastic polyester that boasts a high modulus, high strength and good transparency at room temperature. Therefore, it has raised a lot of interest as a potential replacement for petroleum-based polymers [3]. However, it is challenging to achieve high technical applications due to PLA's brittleness and low heat distortion temperature associated with a T_g around 55 °C and low crystallinity [4-7]. The toughness of PLA can be improved by the incorporation of a rubbery phase. This method is based on the formation of a block or grafted A-B copolymer at the interface between the blend phases during melt mixing. The A-B copolymers can increase the interfacial strengths [8]. Some authors have described ways for improving the toughness of PLA via the reaction of a polymer containing an apposite chemical functionality with the carboxyl or hydroxyl end groups of PLA during melt processing. Functionalized elastomers, such as poly (ethylene-co-glycidyl methacrylate) (EGMA), have been used to toughen PLA [9]. The epoxy group of glycidyl methacrylate (GMA) can react in situ with the carboxyl and hydroxyl end groups of PLA during melt blending and can lead to an EGMA-grafted PLA copolymer that can compatibilize the blend. Therefore, it is expected that glycidyl methacrylate (GMA) grafted poly(ethylene octene) (GPOE) will have a significant toughening effect on PLA. It is usually believed that epoxy groups can react with carboxyl or hydroxyl groups of polyester. The end hydroxyl and/or carboxyl groups of PLA can react with epoxy groups via nucleophilic substitution under appropriate conditions [10].

PLAs contain optically active and crystallizable poly(l-lactic acid) (PLLA) and poly(d-lactide acid) (PDLA), and optically inactive and amorphous poly(dl-lactic acid) (PDLLA) [11,12]. A special crystalline structure termed stereocomplex based on CH_3...C=O interactions of stereoselective van der Waals forces can be formed by blending PLLA and PDLA, which is easily formed by the melt blending, solution casting, or supercritical fluid methods when mixing two polymers with identical chemical composition but different steric structures [13-15]. A homocrystallite of PLLA has a 10_3 helical structure, while the PLLA and PDLA enantiomers crystallize together forming 3_1 helices. This results in a more

*Corresponding author: hlzhang@ciac.ac.cn

compact side by side crystallization for the stereocomplex crystallite [16]. Since Ikada *et al.* found stereocomplexation between enantiomeric PLLA and PDLA [17], numerous studies have been performed for the formation or crystallization, physical properties, crystalline structure, and morphology of the stereocomplex [18-20]. Stereocomplex formation can be easily identified by wide-angle X-ray diffraction (WAXD) and differential scanning calorimetry (DSC). This stereocomplex type poly(lactic acid) (sc-PLA) possesses superior physicomechanical properties such as a melting point of 220-230 °C, which is about 50 °C higher than that of the PLA homopolymer [17,21,22], so that sc-PLA should accordingly have better thermal and mechanical properties and higher hydrolytic stability than PLLA or PDLA. Therefore, PDLA was added to the PLLA/GPOE blends. The purpose of this article is to toughen PLLA, enhance mechanical properties and hydrolytic stability. In this paper, PDLA was added to the PLLA/GPOE blends and the effect of the addition of PDLA was discussed. The mechanical properties, rheological behavior, stereocomplex information, crystalline morphology, enzymatic degradation of PLLA/PDLA/GPOE blends were systematically investigated.

It is expected that the research reported herein is of great help for further improving of the mechanical properties, rheological behavior, and enzymatic degradation of PLLA/PDLA/GPOE blends for future applications.

Experimental

Materials

PLLA (4032D) was used in this study is a commercial product of Nature Works Co. (USA). It exhibited a molecular weight of 207,000 g/mol and a polydispersity of 1.73. D-isomer content of PLLA was approximately 2.0 %. PDLA, synthesized by the ring-opening polymerization of D-lactide [20], was kindly supplied by Professor Chen Xuesi at State Key Laboratory of Polymer Physics and Chemistry, China. It exhibited a weight-average molecular of 110,000 g/mol, polydispersity of 1.92. The GMA grafted POE (GPOE, grafted ratio is 2.5 wt%, chemical structure as shown in Scheme 1) contained 25 % by weight of octene was kindly supplied by Ketong Plastic Co., Ltd. (Shenyang, China).

Processing

Before compounding, both PLLA and PDLA were dried under vacuum at 70 °C for 10 h to remove moisture. PLLA/PDLA/GPOE blends were prepared using a Haake rheomix

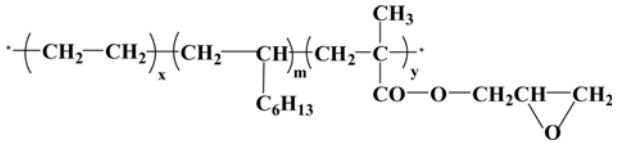

Scheme 1. Structure of GPOE.

Table 1. Compositions of various PLLA/PDLA/GPOE blends

PLLA/PDLA/GPOE (w/w/w)	PLLA (g)	PDLA (g)	GPOE (g)
100/0/0	60.0	0	0
80/0/20	48.0	0	12.0
79/1/20	47.4	0.6	12.0
78/2/20	46.8	1.2	12.0
77/3/20	46.2	1.8	12.0
76/4/20	45.6	2.4	12.0
75/5/20	45.0	3.0	12.0

600 (Karlsruhe, Germany) internal mixer. The melt compounding of PLLA, PDLA, and GPOE was performed at 190 °C for 5 min, the rotor speed was 60 rpm, and the total mixing weight per batch was about 60 g. For comparison, neat PLLA and PLLA/GPOE were treated with the same procedure, respectively. The compositions of the blends are shown in Table 1. After mixing, all the samples were cut into small pieces and then were hot-pressed at 190 °C for 3 min followed by cold-press at room temperature to form the sheets with thickness of 4 mm or 1 mm or 0.1 mm. The compression molding steps were carried out carefully in order to obtain the same treatment for every sample.

Wide Angle X-ray Diffraction (WAXD)

Wide angle X-ray diffraction (WAXD) experiments were performed on a D8 advance X-ray diffractometer (Bruker, Germany) at room temperature in the range of 5-30 ° with a scanning rate of 3 °/min. The Cu K_α radiation (λ=0.15418 nm) source was operated at 40 kV and 200 mA.

DSC Measurements

The melting behaviors of neat PLLA and the blends were investigated with DSC at a heating rate of 10 °C/min from 30 to 240 °C using a DSC Q20 (TA Instruments, USA). The crystallinity of the samples was evaluated from the heat evolved during crystallization by the following relationship:

$$X_c = \frac{\Delta H_f}{w_{PLLA} \times \Delta H_f^0} \times 100\% \quad (1)$$

where ΔH_f is the heat of fusion, ΔH_f^0 is the heat of fusion for 100 % crystalline PLA (93 J/g) [23] and w_{PLLA} is the weight fraction of PLLA.

Dynamic Mechanical Analysis (DMA)

Dynamic mechanical analysis (DMA) was carried out with a dynamic mechanical analyzer SDTA861^e (Mettler Toledo, Switzerland) in the tensile mode. The samples with dimensions of 9×4×1 mm^3 were used. The storage modulus (E') and the dynamic loss factor (tan δ) were determined at a frequency of 1 Hz and a heating rate of 3 °C/min as a function of temperature from 0 to 115 °C.

Crystalline Morphology

The crystallite morphology of PLLA/PDLA/GPOE samples was observed with a Leica DMLP polarized microscope (POM) (Wetzlar, Germany) equipped with a Linkam TM600 hot stage and a computer-controlled charged-coupled-device camera. A small amount of sample with a thickness of approximately 20 μm was placed between two microscope cover glasses and then placed on the hot stage. The samples were heated from room temperature to 190 °C at a rate of 30 °C/min, and maintained at this temperature for 3 min to eliminate any thermal history, and then quenched to 130 °C at a rate of 45 °C/min for isothermal crystallization and held for 30 min. The morphology changes were recorded during the crystallization process.

Rheological Behavior

Dynamic rheological experiments were carried out on a AR2000EX rheometer (TA Instruments, USA) in a plate-plate configuration (25 mm in diameter and 1 mm in gap) at 190 °C. The sheet samples were about 1.0 mm in thickness. The samples were examined in a frequency-sweep mode, from 100 to 0.1 rad/s, with a constant strain of 1.25 %.

Mechanical Properties Test

Uniaxial tensile tests were carried out on dumbbell shaped specimens (W×H×L=4.0×1.0×20.0 mm^3), which were punched out from the compression-molded sheets. The measurements were performed using a tensile-testing machine (Instron Corporation, USA) according to ASTM D638-2008 at a crosshead speed of 20 mm/min. All tests were carried out at room temperature and 50 % relative humidity. At least five specimens were tested for each sample to get an average value.

Notched Izod impact tests were performed at 23±2 °C according to ASTM D256-2010 on an impact testing machine (Changchun City Intelligent Instrument Equipment Co., Ltd., China). The samples with dimensions 80.0×10.0×4.0 mm^3 were obtained from compression-molded specimens. The notch was milled in having a depth of 2.54 mm, an angle of 45 °, and a notch radius of 0.25 mm.

Scanning Electron Microscopy (SEM)

The morphology of the composites was observed using a field emission scanning electron microscopy (SEM) (XL30 ESEM FEG, FEI Co., Eindhoven, The Netherlands) at an accelerating voltage of 10 kV. The samples were immersed in liquid nitrogen for about 3 min, and then broke off. The cryo-fractured surfaces of the samples were coated with a thin layer of gold and then SEM micrographs recorded in order to evaluate the dispersion of the rubber particles in the PLLA matrix.

Enzymatic Hydrolysis

The enzymatic degradation of the blend films for PLLA was carried out in Tris-HCl buffered solution (pH=8.0) containing 0.2 mg ml^{-1} of proteinase K (Genview) at 45 °C with shaking at 140 rpm. Sample films (10×10×0.1 mm^3) were placed in small glass bottles filled with 1.5 m*l* Tris-HCl buffered solution containing proteinase K. The films were periodically removed, washed with distilled water, and dried to a constant weight in a vacuum before weight analysis. For each polymer sample, three films were used, and the average value of their weight loss was reported.

Results and Discussion

Stereocomplex Formation

To acquire additional information on the crystallization behaviors of sc-PLA, the crystalline structure of the PLLA materials was characterized by WAXD. Figure 1 shows the WAXD patterns and DSC melting curves of these prepared

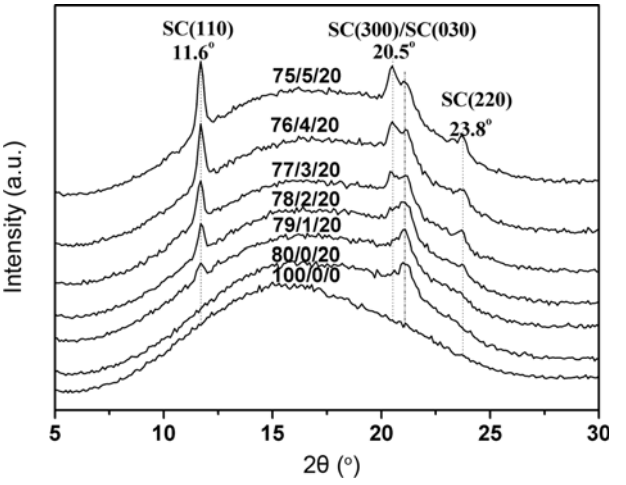

Figure 1. WAXD profiles of PLLA/PDLA/GPOE blends showing the formation of sc-PLA.

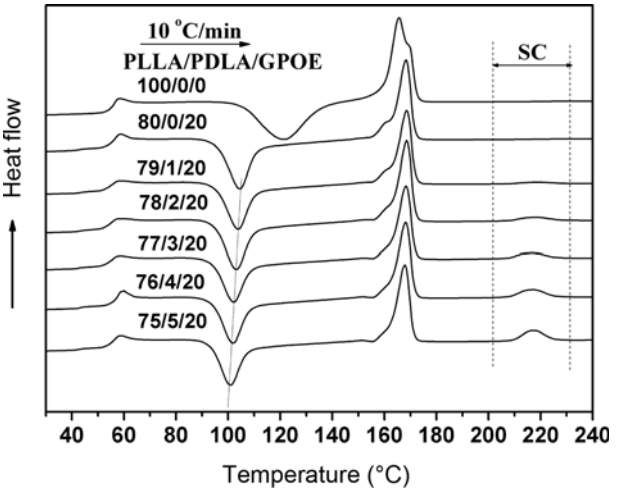

Figure 2. DSC curves of PLLA/PDLA/GPOE blends in the first heating.

Table 2. Thermal properties of PLLA/PDLA/GPOE blends

PLLA/PDLA/GPOE (w/w/w)	PLLA						sc-PLA	sc-PLA
	T_g (°C)	T_{cc} (°C)	ΔH_{cc} (J/g)	T_m (°C)	ΔH_f (J/g)	X_c (%)	T_m (°C)	ΔH_f (J/g)
100/0/0	56.4	122.0	43.9	165.6	43.3	46.6	-	-
80/0/20	56.1	104.3	31.5	168.3	33.2	44.6	-	-
79/1/20	55.6	103.9	31.6	168.5	32.1	43.7	217.1	1.4
78/2/20	55.7	103.2	29.2	168.5	31.1	42.9	217.2	3.0
77/3/20	55.5	102.1	27.4	168.3	29.5	41.2	217.5	4.5
76/4/20	55.3	101.6	26.5	168.2	28.4	40.1	217.3	5.5
75/5/20	55.4	100.9	25.4	167.7	27.2	39.0	217.1	6.4

samples. In Figure 1, all WAXD patterns do not exhibit diffraction peaks of PLLA homocrystallites at 2θ values of 16°, 18.4°, and 21.8° [24] indicating no homocrystallites existed, and neat PLLA was amorphous. In the PLLA/GPOE blend, the reflection peak at 2θ value of 21.1° belonged to GPOE. A weak but still visible diffraction peak appears at 2θ value of 11.6°, corresponding to the (110) planes of SC crystallites [22]. Increasing the concentration of PDLA to be above 1 wt%, other two diffraction peaks of SC crystallites appear at 2θ value of 20.5° and 23.8°, assigned to the (300) and/or (030) planes and (220) planes of SC crystallites [22]. These peaks become stronger with increasing PDLA concentration.

The stereocomplexation behavior of blends was further studied by using DSC. The melting peaks of sc-PLA crystallites at around 217 °C could be observed in Figure 2 for the blends, the area of the melting endotherm for the stereocomplex increased as the amounts of PDLA in the blend increased. It agreed well with the results of WAXD. Table 2 shows various DSC parameters of neat PLLA, PLLA/GPOE, PLLA/PDLA/GPOE blends. Compared to neat PLLA, the cold crystallization temperature of PLLA decreased from 122 °C to 104 °C by the incorporation of GPOE at 20 %. This indicated that GPOE may act as a role of nucleation agent. Pure PLLA showed a main melting peak at 165.0 °C and a shoulder at 169.5 °C. During the DSC heating scan of pure PLLA, it can be suggested that some of the less perfect crystals had enough time to melt and reorganize into crystals with higher structural perfection (thicker lamellae), more stable crystals, and then remelt at higher temperature [25-27]. In all of the samples, three other transitions including the glass transition, the cold crystallization, and melting peak from the PLLA homopolymer are present around 56 °C, 100 °C, and 168 °C, respectively. The glass transition temperatures and the melting temperatures of homocrystallites seem to be not affected by the addition of PDLA or the formed SC crystallites. The cold crystallization peak temperature decreases with increasing concentration of PDLA, indicating exactly the effect of the formed SC crystallites on the crystallization of PLLA. The area of the melting endotherm for the stereocomplex crystals increased as the amount of PDLA in the blend increased showing that

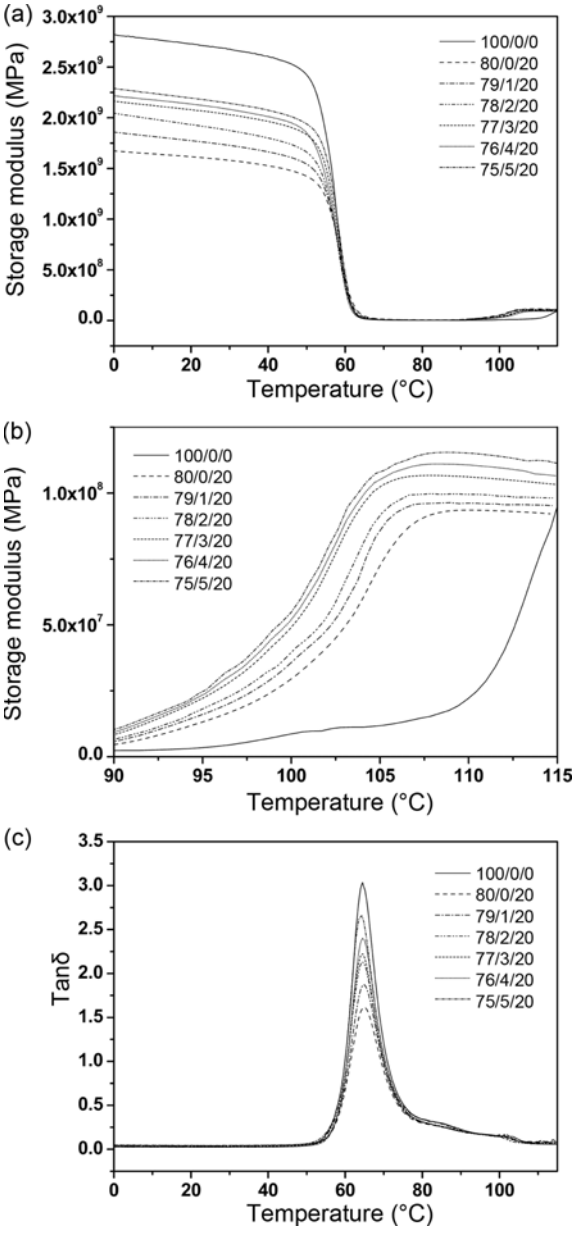

Figure 3. Temperature dependence of (a) storage modulus, (b) magnification of storage modulus in the range of 90 to 115 °C, and (c) tan δ for the neat PLLA and its composites.

the initial composition of the blend can be used to control the amount of stereocomplex in the final material.

Dynamic Mechanical Analysis (DMA)

Results of dynamic mechanical analysis carried out over a range of temperatures at a constant frequency of 1 Hz are shown in Figure 3. It is clear from storage modulus (E') versus temperature curves (Figure 3(a)) that E' of neat PLLA was the highest than those of the blends throughout the temperature range from 0 to 50 °C. In addition, compared with PLLA/GPOE blend, E' of PLLA/PDLA/GPOE blends increased with increasing PDLA content at the same temperature range, indicating that the sc-PLA had a strong influence on the elastic properties of the PLLA matrix. This result was in good agreement with the result of tensile mechanical testing. For all the samples, the E' decreased sharply in the range of 50 to 60 °C due to the glass transition of PLLA. Above the cold crystallization temperature (T_{cc}), the enhancement of E' is slight in the PLLA blends. Then the E' rose from about 90 to 115 °C due to the cold crystallization of PLLA. With the addition of GPOE and PDLA/GPOE, the temperature at which E' started to increase shifted to a lower

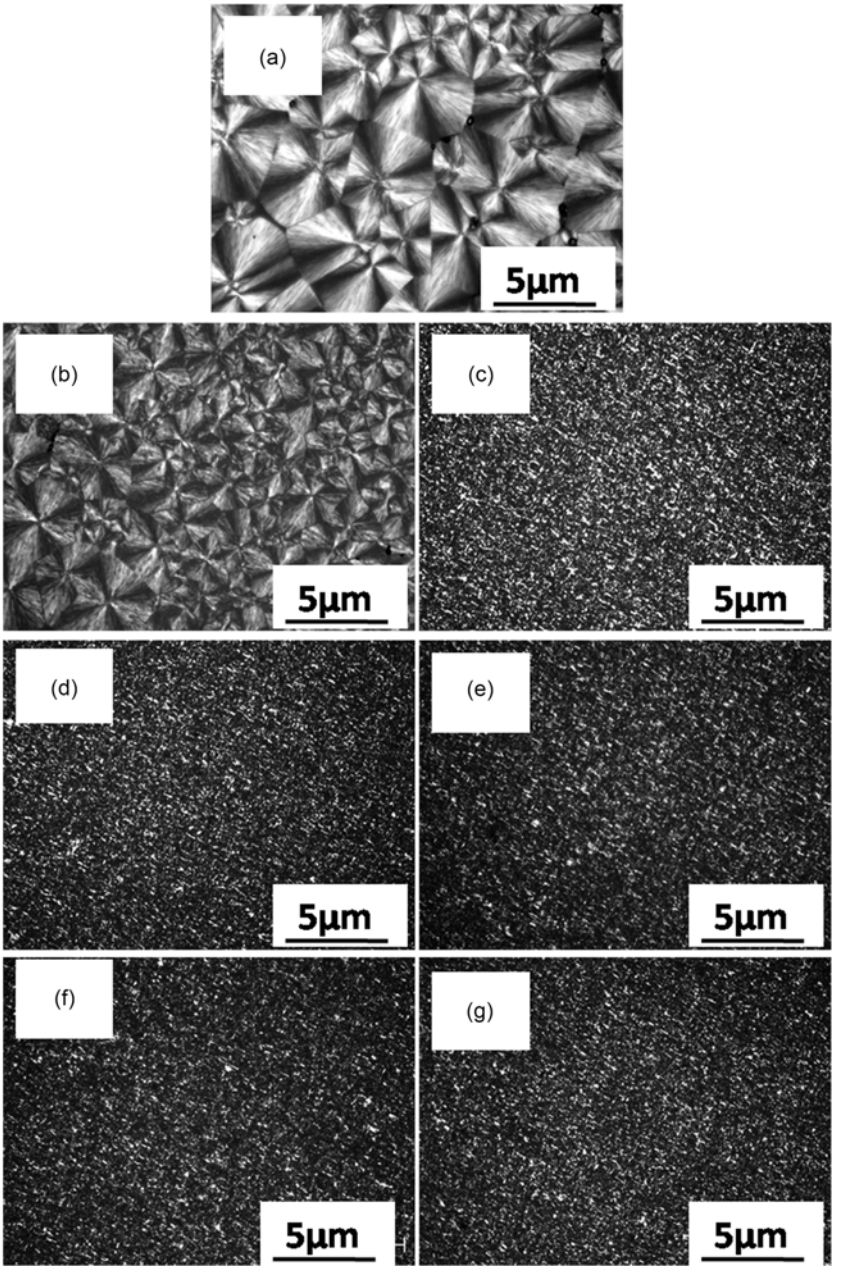

Figure 4. POM images of PLLA/PDLA/GPOE blends; (a) 100/0/0, (b) 80/0/20, (c) 79/1/20, (d) 78/2/20, (e) 77/3/20, (f) 76/4/20, and (g) 75/5/20 at 130 °C for 30 min.

temperature. The result suggested that the incorporation of PDLA enhanced the cold-crystallization ability of PLLA and therefore decreased the cold-crystallization temperature of PLLA in the blend. Consequently, the thermal stability of PLLA enhanced to a higher temperature. In addition, from Figure 3(c), we can find that the peak position tan δ does not shift which means that the T_g of PLLA does not change obviously. This result is in accordance with the result of DSC test.

Crystalline Morphology

Spherulitic morphology of neat PLLA, PLLA/GPOE, and PLLA/PDLA/GPOE blends was studied with POM. Figure 4 displays the spherulitic morphology of neat PLLA, PLLA/GPOE, and PLLA/PDLA/GPOE blends isothermally crystallized at 130 °C for 30 min. Figure 4(a) shows that the well-developed spherulites grow to a size of about 5 μm in diameter, and the boundaries can be seen clearly for neat PLLA and PLLA/GPOE samples. Figure 4(c)-(g) illustrate the POM images of the blends with the PDLA loading for 1, 2, 3, 4 and 5 wt%. The presence of PDLA in the PLLA/GPOE blends resulted in smaller size of spherulites and obscurer spherulite boundaries. This phenomenon indicated that PDLA might be due to the heterogeneous nucleation agent effect of in situ formed stereocomplex crystals. However, the content of PDLA in the blends did not show obvious effect on the morphology of spherulites.

Rheological Properties

Viscoelastic response of the neat PLLA, PLLA/GPOE and PLLA/PDLA/GPOE blends was investigated by oscillatory shear rheological measurements at 190 °C. At such a temperature, the PLLA matrix (T_m~165 °C) is in a molten state whereas the SC-PLA (T_m~230 °C) is still in the rigid crystalline form. The dependence of the storage modulus (G') on the angular frequency PLLA/GPOE/PDLA blends is shown in Figure 4. The dynamic storage modulus related to the elastic character of the blends or the energy stored during the deformation. As shown in Figure 5, the storage modulus (G') of all samples increases as the frequency increases. At low frequencies, compared with that of neat PLLA, the storage modulus of the PLLA/GPOE blend increased by about an order of magnitude. The higher absolute values of dynamic modulus indicated the formation of interaction and entangled structures between the PLLA chains and the chains of polyolefin elastomer [28-30]. In addition, the interactions among the sc-PLA phase were rigid strong enough, and as a result led to increasing of G' with sc-PLA content.

Figure 6 displayed the relationship between complex viscosity η* and angular frequency of the PLLA, PLLA/GPOE and PLLA/PDLA/GPOE blends at 190 °C. The addition of sc-PLA resulted in the gradual increase in the viscosity of the blends. Complex viscosity η* of pure PLLA

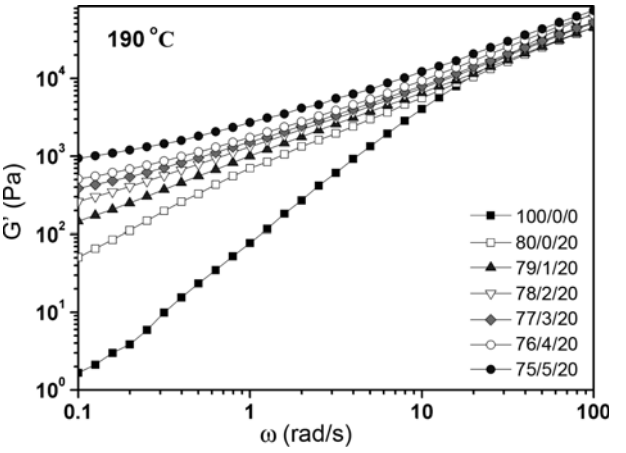

Figure 5. Dynamic storage (G') versus frequency for the neat PLLA and its composites.

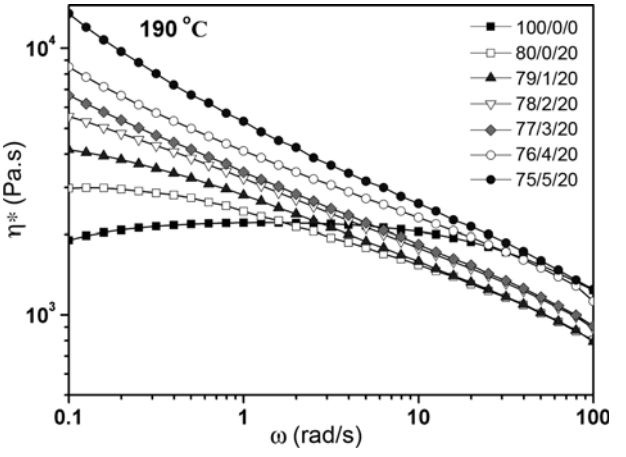

Figure 6. Plots of complex viscosity (η*) versus frequency for the neat PLLA and its composites.

displays a Newton liquid behavior at frequency range of ~0.4-10 rad/s. In other words, it is constant with the frequency increasing up to 10 rad/s where the shear-thinning behavior of η* appears. It was seen that neat PLLA sample showed typical terminal behavior at low frequencies with the scaling properties of $G' \propto \omega^2$, which was in consistent with the linear viscoelastic theory. Comparing to PLLA melt, the complex viscosity η* of PLLA/GPOE melt display strong shear-thinning tendency at all frequencies and tendency becomes stronger with the increasing of sc-PLA content. What is more, regardless of frequency, complex viscosity η* increased monotonically with increasing sc-PLA content in the blends. Due to the blending, subsequent processing, and characterization temperature far below the melting point of sc-PLA, the sc-PLA phase in the blends could not be melted. Therefore, it is expected that these sc-PLA sphere structures formed in situ can reinforce the melt blending in a relatively wider temperature range. Dynamic rheological properties

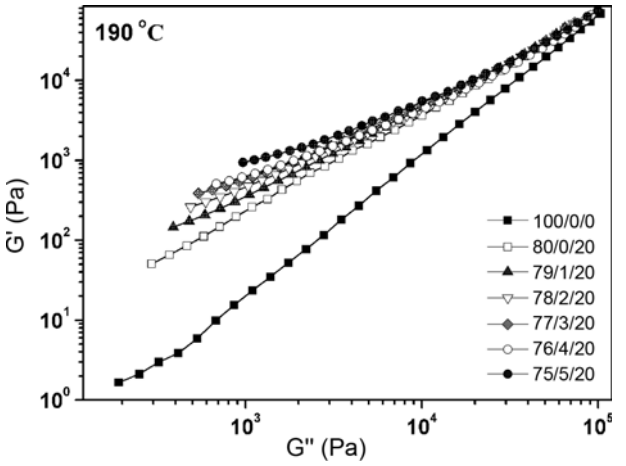

Figure 7. The plots of dynamic storage modulus (G') versus dynamic loss modulus (G'') at 190 °C for neat PLLA and its composites.

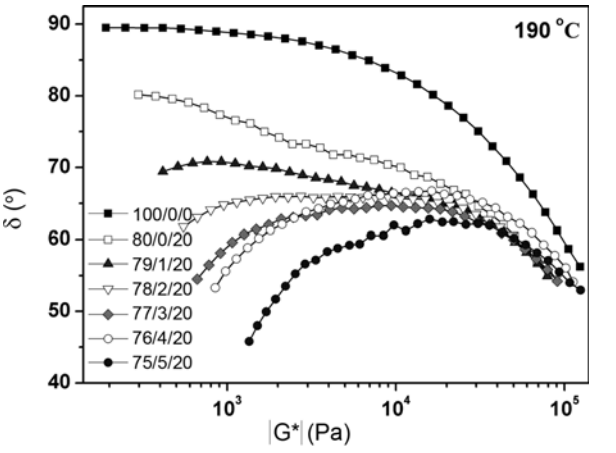

Figure 8. Phase angle versus $|G^*|$ plots of neat PLLA and its composites.

are highly sensitive to structure and interactions within the polymer melt. In PLLA/PDLA/GPOE melt, sc crystal forms a large number of tiny solid particles, and the molecular chain is subjected to shearing and sliding friction, the required external force is larger, so that the viscosity of the material is improved. It is also possible that due to the interactions among the three components, the degree of branching of the molecular chain becomes larger, and the formation of entanglements among PLLA, PDLA, and GPOE macromolecular chains becomes strong.

As soon as the composites percolated, the large scale polymer chain relaxation behaviors might be highly affected by the percolated sc-PLA network. Figure 7 shows the plots of dynamic storage modulus (G') versus dynamic loss modulus (G'') [31] for neat PLLA and its composites at 190 °C, respectively. In addition, the reduced slope with the addition of sc-PLA indicated that the composites became more heterogeneous. It should be noted that the inflection point where the slope was changed shifts to a higher frequency with an increase in sc-PLA loadings. This indicated that much energy was needed for the polymer relaxation process.

Rheological data can be presented by plotting the phase angle versus the absolute value of the complex modulus. The δ-$|G^*|$ curves of neat PLLA and its composites at 190 °C are plotted in Figure 8. This plot is the so-called van Gurp-Palmen plot, which may be pointed out that this plot provides other application to analyze rheological behavior of polymer melts. The van Gurp-Palmen plots were used as a tool to investigate compatibilization of blends by Macaubas, Demarquette, and Schulze *et al*. [32,33] In general, the curve of the homogeneous linear polymer melt finally reaches a plateau at 90 ° when going from high to low complex modulus $|G^*|$ values. In this study, the low-frequency phase angle of the neat PLLA sample is close to 90 °, which indicated a flow behavior presented by the viscoelastic fluid. In contrast to that, such plots of the two-phase samples (PLLA/GPOE blend) exhibit characteristic shapes in low complex modulus $|G^*|$ regions. The phase-separated samples of symmetric composition pass a maximum and then descend with decreasing complex modulus $|G^*|$. As the PDLA loadings increase from 1 % to 5 wt%, the low-frequency decreases from 68° to 45 °, indicating a rheological fluid-solid transition and an enhanced elastic behavior in that ternary system. Therefore, the enhanced elastic behavior and melt strength may be good for the actual production process.

Mechanical Properties

The tensile properties of neat PLLA, PLLA/GPOE, and PLLA/PDLA/GPOE blends are given in Table 3. The tensile strength and the elongation at break of neat PLLA were 64.4 MPa and 4.1 %, respectively. The addition of GPOE led to tensile strength decreased, while elongation at break and impact strength increased. Then adding PDLA formed sc-PLA with content 1-5 %. The increases in tensile strength and modulus were direct consequences of the suppression of the global cooperative chain movement of the PLLA by the percolated sc-PLA network structure. It was noted that the

Table 3. Mechanical properties of PLLA/PDLA/GPOE blends

PLLA/PDLA/GPOE (w/w/w)	Tensile strength (MPa)	Elongation at break (%)	Young's modulus (MPa)	Notched impact strength (kJ/m^2)
100/0/0	64.4±1.7	4.1±0.8	1857±121	2.1±0.3
80/0/20	32.4±1.2	149.9±13.4	1034±134	52.5±1.2
79/1/20	33.1±1.1	95.3±3.6	1154±115	54.7±1.4
78/2/20	34.8±1.4	90.8±2.5	1205±106	53.7±1.0
77/3/20	35.7±1.0	73.5±7.2	1214±104	48.3±1.3
76/4/20	37.4±1.5	50.3±6.8	1218±109	43.8±1.2
75/5/20	38.5±1.4	36.4±4.3	1223±102	41.4±1.6

reinforcing effect increased with sc-PLA content in the blend, while elongation at break decreased. Although sc-PLA only existed as particulate fillers in blends, such fillers still exerted a significant restriction to the chain movement of PLLA, resulting in significant increases in tensile strength and modulus and a decrease in elongation at break. However, 80/20 PLLA/GPOE, 79/1/20 PLLA/PDLA/GPOE, and 78/2/20 PLLA/PDLA/GPOE blends still showed fairly good ductility. However, due to a higher melting point of sc-PLA (217 °C) compared with PLLA (165 °C), in situ formed sc-PLA can reinforce the PLLA/GPOE in a wider temperature window, which will extend PLLA processing methods, like film blowing and foaming.

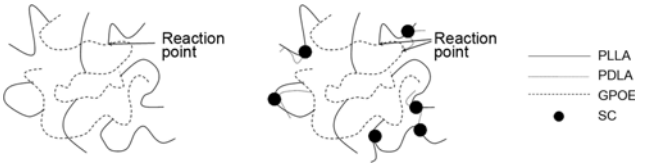

Figure 9. The interaction mechanism diagram of PLLA, PDLA and GPOE.

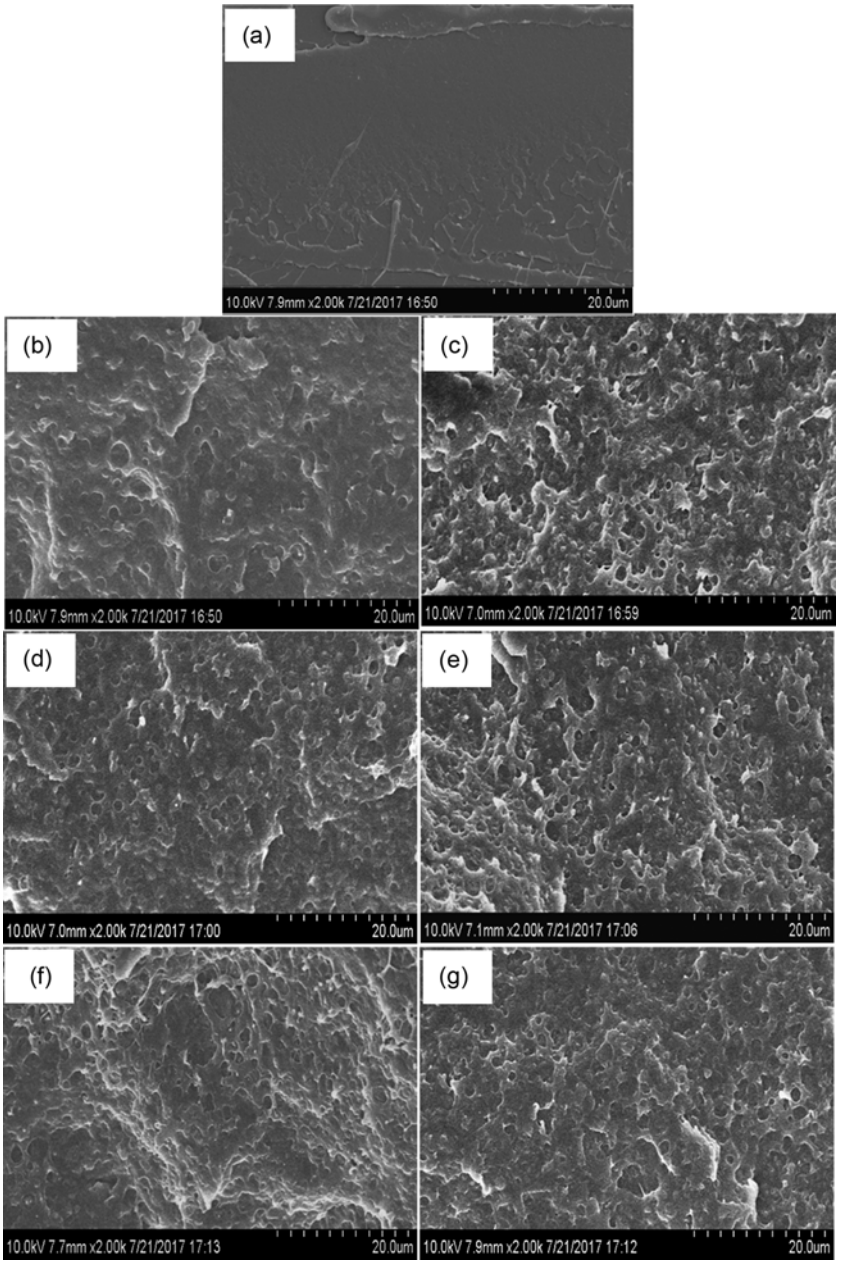

Figure 10. The SEM micrographs of cryo-fractured surfaces of PLLA/PDLA/GPOE blends; (a) 100/0/0, (b) 80/0/20, (c) 79/1/20, (d) 78/2/20, (e) 77/3/20, (f) 76/4/20, and (g) 75/5/20.

The impact strength evaluation is important in the investigation of the fracture toughness of polymer blends. The results of the notched Izod impact strength of the neat PLLA and its blends are also given in Table 3. The virgin PLLA is very fragile, its impact strength is only 2.1 kJ/m^2. The impact strength of PLLA/GPOE blends were about 25 times than that of neat PLLA. As for the 79/1/20 and 78/2/20 PLLA/PDLA/GPOE blends, the notched impact strength of 54.6 and 53.7 kJ/m^2 was achieved, respectively. This result illustrated that the addition of PDLA has further strengthened the force between the elastomer and the PLLA matrix. The interaction mechanism diagram of PLLA, PDLA, and GPOE was shown in Figure 9. However, when the PDLA content was over 2 wt% in the PLLA/PDLA/GPOE blends, the notched impact strength of the blends decreased from 48.3 to 41.4 kJ/m^2 lower than that 52.5 kJ/m^2 of PLLA/GPOE. A possible explanation is that the binding force between the elastomer and the PLLA matrix is too large, making against the transfer of stress, hindering the occurrence and growth of the craze. At the same time, the formation of the SC crystal is brittle, a large number of SC crystal will make the impact strength of material decline again.

Scanning Electron Microscopy (SEM)

It is usually believed that the dispersion of components in a given polymer matrix is one of the most significant factors influencing the physical properties of the material. When the GPOE particles were dispersed in PLLA, mechanical properties of PLLA were effectively improved. To follow the dispersion of GPOE in the PLLA matrix, the cryo-fractured surfaces of the PLLA/PDLA/GPOE blends were observed by SEM. The morphologies of the PLLA, PLLA/GPOE, and PLLA/PDLA/GPOE blends are shown in Figure 10. A typical brittle fractured surface, which is rather smooth, of PLLA can be observed in Figure 10(a). The fractured surface of the neat PLA revealed its nature of weak resistance to crack initiation and propagation. While for the blends with the addition of GPOE, it can be clearly found that the surface of the blends changes obviously. The surfaces of the PLLA/PDLA/GPOE blends tended to be increasingly coarser compared with the that of pure PLLA. However, for all the PLLA/PDLA/GPOE blends, there was no massive matrix yielding on the surface as can be seen in Figure 10(b)-(g). Only layered structures and ductile surfaces were founded on the surface. It is thought that GPOE in PLLA can absorb the energy, when the outside force loaded on the blends and lead to plastic deformation, cause stress concentration because of its different moduli compared with that of PLLA. The GPOE can evenly disperse in the PLLA matrix. The addition of PDLA in the blends would not influence the dispersion of GPOE particles.

Enzymatic Hydrolysis

The biodegradability of PLLA/PDLA/GPOE composites is extremely important for the potential application of the materials in the future. Proteinase K (EC 3.4.21.14) is a well-known enzyme to catalyze hydrolysis of PLA when PLA contains sufficiently long L-lactide (LLA) unit sequences in the amorphous phase [34-41]. Figure 11 shows the weight loss profiles of PLLA/PDLA/GPOE blend films as a function of time during the proteinase K-catalyzed degradation. The weight loss of the films increased with time for all samples. The rate of enzymatic degradation could be determined from the slope of the weight loss against time. As we known, the rate of enzymatic hydrolysis of biodegradable materials was dependent on the degree of crystallinity [42-46]. Many results demonstrated that the amorphous region of PLLA degraded more easily than crystalline region of PLLA. What is more, the degradation rate increased with the decrease of crystallinity (X_c) of PLLA. From Table 2, the virgin PLLA displayed the crystallinity of 46.6 %. In addition, it should be noted that the degree values of PLLA component in the composites decreased from 44.6 to 39.0 with the incorporation 20 % GPOE and 1-5 % PDLA. This result led to the acceleration of PLLA hydrolysis there, thereby acceleration degradation.

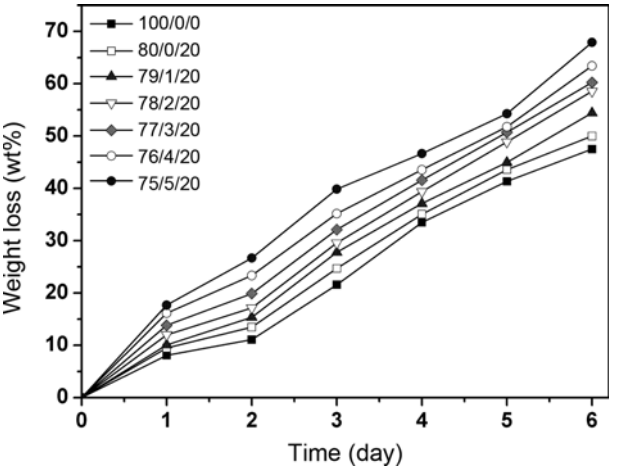

Figure 11. PLLA weight loss profiles of PLLA/PDLA/GPOE blends films as a function of time during the proteinase K-catalyzed degradation.

Conclusion

The composites of PLLA/PDLA/GPOE with different PDLA loadings were prepared via melt compounding to investigate the effects of sc-PLA loadings on the stereocomplex formation, crystalline morphology, viscoelasticity, mechanical, and enzymatic hydrolysis properties. The formation of stereocomplex was proved by WAXD and DSC. The POM results showed that more PLLA spherulites were formed in the PLLA/PDLA/GPOE blends than those in the PLLA/GPOE blend. Moreover, the size of PLLA spherulites of the PLLA/PDLA/GPOE blends is smaller than

that of the PLLA/GPOE blend. The increased nucleation density of PLLA spherulites in the blends indicates that stereocomplex crystals formed in situ may act as an effective nucleating agent during the crystallization process of PLLA/GPOE blend. Static mechanical properties show that with the increase in PDLA content, the tensile strength and modulus of the PLLA/PDLA/GPOE blends increased, indicating that significant reinforcement effect was achieved by adding sc-PLA. DMA test indicated the same mechanical results. However, the elongation at break decreased with the increase of the sc-PLA due to the hindered mobility and orientation of the PLLA macromolecular chains during tension. By adding 1-2 wt% PDLA, the ternary system has better tensile and impact properties. SEM images indicated that with the addition of GPOE, the surface became much more coarser than PLLA. Investigation on the rheological properties of the melts embedded by SC crystallites showed that the presence of the formed SC crystallites can reinforce the PLLA melt due to the filler effect and cross-linking effect of SC. Moreover, a transition from the liquid-like to solid-like viscoelastic behaviors was observed, which exactly reveals the existence of the SC crystallite network in the melt. Moreover, the biodegradability of PLLA/PDLA/GPOE composites illustrated that the formation of sc-PLA promoted degradation.

Acknowledgement

This work was supported by the fund of Science & Technology Bureau of Jilin Province of China (No. 20160307001GX), Science & Technology Bureau of Changchun City of China (No. 16SS03), Development and Reform commission of Jilin Province of China (No. 2015Y027), and Science & Technology Bureau of Jilin City of China (No. 20163206).

References

1. K. Madhavan Nampoothiri, N. R. Nair, and R. P. John, *Bioresour. Technol.*, **101**, 8493 (2010).
2. S. H. Lee and S. Y. Yeo, *Fiber. Polym.*, **17**, 1154 (2016).
3. R. Auras, B. Harte, and S. Selke, *Macromol. Biosci.*, **4**, 835 (2004).
4. J. K. Kim, D. J. Park, M. S. Lee, and K. J. Ihn, *Polymer,* **42**, 7429 (2001).
5. O. Martin and L. Averous, *Polymer*, **42**, 6209 (2001).
6. R. M. Rasal, A. V. Janorkar, and D. E. Hirt, *Prog. Polym. Sci.,* **35**, 338 (2010).
7. M. HiljanenVainio, T. Karjalainen, and J. Seppala, *J. Appl. Polym. Sci.,* **59**, 1281 (1996).
8. S. L. Sun, M. Y. Zhang, H. X. Zhang, and X. M. Zhang, *J. Appl. Polym. Sci.,* **122**, 2992 (2011).
9. H. T. Oyama, *Polymer,* **50**, 747 (2009).
10. Y. Zhao, Y. Zhang, Z. L. Li, H. W. Pan, Q. L. Dong, L. J. Han, H. L. Zhang, and L. S. Dong, *Korean. J. Chem. Eng.*, **33**, 1104 (2016).
11. H. Tsuji, *Biomaterials*, **24**, 537 (2003).
12. A. Sodergard and M. Stolt, *Prog. Polym. Sci.*, **27**, 1123 (2002).
13. J. Slager and A. J. Domb, *Adv. Drug. Deliver. Rev.*, **55**, 549 (2003).
14. J. Slager, M. Gladnikoff, and A. J. Domb, *Macromol. Symp.*, **175**, 105 (2001).
15. H. Tsuji and Y. Ikada, *Macromolecules*, **26**, 6918 (1993).
16. S. R. Andersson, M. Hakkarainen, S. Inkinen, A. Sodergard, and A. C. Albertsson, *Biomacromolecules*, **13**, 1212 (2012).
17. Y. Ikada, K. Jamshidi, H. Tsuji, and S. H. Hyon, *Macromolecules*, **20**, 904 (1987).
18. X. F. Wei, R. Y. Bao, Z. Q. Cao, W. Yang, B. H. Xie, and M. B. Yang, *Macromolecules*, **47**, 1439 (2014).
19. Y. Li, C. Y. Han, X. Zhang, Q. L. Dong, and L. S. Dong, *Thermochim. Acta*, **573**, 193 (2013).
20. H. Tsuji, *Macromol. Biosci.*, **5**, 569 (2005).
21. H. Tsuji, S. H. Hyon, and Y. Ikada, *Macromolecules*, **24**, 5657 (1991).
22. H. Tsuji, S. H. Hyon, and Y. Ikada, *Macromolecules*, **24**, 5651 (1991).
23. Z. Su, Q. Li, Y. Liu, G. Hu, and C. Wu, *Eur. Polym. J.*, **45**, 2428 (2009).
24. L. Cartier, T. Okihara, and B. Lotz, *Macromolecules*, **30**, 6313 (1997).
25. R. M. Taib, Z. A. Ghaleb, and Z. A. Mohd Ishak, *J. Appl. Polym. Sci.,* **123**, 2715 (2012).
26. L. Jiang, M. P. Wolcott, and J. W. Zhang, *Biomacromolecules*, **7**, 199 (2006).
27. R. Wang, S. Wang, Y. Zhang, C. Wan, and P. Ma, *Polym. Eng. Sci.*, **49**, 26 (2009).
28. Y. L. Feng, Y. X. Hu, J. H. Yin, G. Y. Zhao, and W. Jiang, *Polym. Eng. Sci.*, **53**, 389 (2013).
29. Y. P. Hao, H. Y. Liang, J. J. Bian, S. L. Sun, H. L. Zhang, and L. S. Dong, *Polym. Int.*, **63**, 660 (2014).
30. H. L. Zhang, N. A. Liu, X. H. Ran, C. Y. Han, L. J. Han, Y. G. Zhuang, and L. S. Dong, *J. Appl. Polym. Sci.*, **125**, E550 (2012).
31. C. D. Han and J. K. Kim, *Polymer*, **34**, 6209 (1993).
32. P. H. P. MacAubas and N. R. Demarquette, *Polym. Eng. Sci.*, **42**, 1509 (2002).
33. D. Schulze, T. Roths, and C. Friedrich, *Rheol. Acta*, **44**, 485 (2005).
34. H. Tsuji and S. Miyauchi, *Polymer*, **42**, 4463 (2001).
35. H. Tsuji and S. Miyauchi, *Polym. Degrad. Stabil.*, **71**, 415 (2001).
36. S. M. Li, M. Tenon, H. Garreau, C. Braud, and M. Vert, *Polym. Degrad. Stabil.*, **67**, 85 (2000).
37. S. M. Li and S. McCarthy, *Macromolecules*, **32**, 4454 (1999).
38. R. T. MacDonald, S. P. McCarthy, and R. A. Gross, *Macromolecules*, **29**, 7356 (1996).

39. M. S. Reeve, S. P. McCarthy, M. J. Downey, and R. A. Gross, *Macromolecules*, **27**, 825 (1994).
40. H. Tsuji and S. Miyauchi, *Biomacromolecules*, **2**, 597 (2001).
41. H. Cai, V. Dave, R. A. Gross, and S. P. McCarthy, *J. Polym. Sci. Pol. Phys.*, **34**, 2701 (1996).
42. M. H. Rahaman and H. Tsuji, *Polym. Degrad. Stabil.*, **98**, 709 (2013).
43. A. Sodergard, J. F. Selin, and J. H. Nasman, *Polym. Degrad. Stabil.*, **51**, 351 (1996).
44. H. Tsuji and Y. Ikada, *Polym. Degrad. Stabil.*, **67**, 179 (2000).
45. H. Tsuji and Y. Ikada, *J. Polym. Sci. Pol. Chem.*, **36**, 59 (1998).
46. S. M. Li, H. Garreau, and M. Vert, *J. Mater. Sci. Mater. M.*, **1**, 198 (1990).